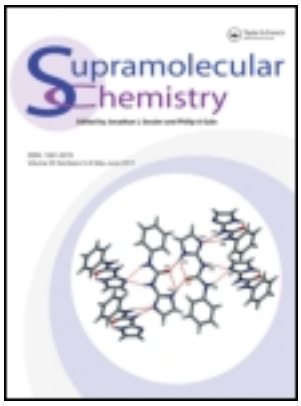

Supramolecular Chemistry
Publication details, including instructions for authors and subscription information:
http://www.tandfonline.com/loi/gsch20

Membrane activity of 3-hydroxyglutarate diesters

Kathleen Genge [a], Joanne M. Moszynski [a], Matthew Thompson [a] & Thomas M. Fyles [a]
[a] Department of Chemistry, University of Victoria, Victoria, BC, V8W 3V6, Canada

Available online: 26 Oct 2011

To cite this article: Kathleen Genge, Joanne M. Moszynski, Matthew Thompson & Thomas M. Fyles (2012): Membrane activity of 3-hydroxyglutarate diesters, Supramolecular Chemistry, 24:1, 29-39

To link to this article: http://dx.doi.org/10.1080/10610278.2011.622382

Supramolecular Chemistry
Vol. 24, No. 1, January 2012, 29–39

Taylor & Francis
Taylor & Francis Group

Membrane activity of 3-hydroxyglutarate diesters

Kathleen Genge, Joanne M. Moszynski, Matthew Thompson and Thomas M. Fyles*

Department of Chemistry, University of Victoria, Victoria, BC V8W 3V6, Canada

(*Received 10 June 2011; final version received 25 August 2011*)

The synthesis and characterisation of the transport activity and membrane localisation of three 3-hydroxyglutarate diesters containing saturated and diphenylacetylene-derived groups are described. In bilayer vesicles and planar bilayers, the two compounds bearing a terminal carboxylic acid form active ion channels; a related neutral compound is inactive. Nonlinear current–voltage behaviour is observed for the active diphenylacetylene-derived diester. The transport activity occurs at concentrations that are substantially below the level at which the compounds aggregate. Diphenylacetylene-derived fluorescence allows the partitioning and the aggregation states of the compounds to be probed. It is clear that the active compounds do not simply act as detergents, but form defined, if irregular, ion channels in the membrane.

Keywords: synthetic ion channel; fluorescence; vesicle; bilayer membrane

Introduction

Numerous synthetic ion channel-forming compounds have been reported in the past three decades (reviews *1–7*). Although functionally similar in that they open ion-conducting pathways in bilayer membranes, the diversity of structures is remarkable. In recent years, some examples have been shown to act as novel antibiotics (*8–11*), and others have led to new types of sensors (*12*, *13*). In the long term, such practical applications will require relatively simple syntheses and relatively simple compounds, so one enduring motivation has been to identify 'minimalist' structures. Significant milestones in this regard are the ion-pair systems reported by Kobuke and co-workers (*14*), linear oligoethyleneglycol esters reported by Schäfer, Neumann and co-workers (*15*), the isophthalate ethers we reported (*16*) and more recent reports of isophthalamides by the Yang group (*8*, *9*) and isopicolinamides by Gokel and co-workers (*17*). Underlying this series of papers are the puzzling and poorly reproducible channels formed by the detergent Triton X 100 (*18*, *19*). Whatever the structural origins of the activities of these simple compounds might be, it is abundantly clear that simple compounds can act as effective ion channels.

In previous published work on the solid phase synthesis methodology used to prepare linear oligoesters, a glutaratediester compound HO_2C-***Dod-G(12)***-OH[1] was prepared as representative of one type of expected impurity of the method (*20*). An isomeric compound HO_2C-***G(12)-Dod***-OH was also prepared as part of the methodology development. Although the second of these 'dimers' was inactive as a transporter, the former compound showed considerable activity in the vesicle assay. At the time this was dismissed as simply due to a detergent-like action of this small molecule and was not examined further (*20*). As the activity of this class of compounds was explored further (*21*, *22*), the activity of HO_2C-***Dod-G(12)***-OH and the inactivity of the positional isomer remained an unresolved question. Is this compound a detergent that showed activity only because it promoted vesicle lysis? Or is this compound an active ion channel-forming compound of unusually simple structure?

More recent work on the use of a diphenylacetylene unit as a fluorescent probe in other oligoester channel compounds has allowed the localisation and activity of the oligoesters to be probed in detail and has placed a focus on the aggregation of compounds in aqueous solution (*23*). We were therefore prompted to re-examine the activity of simple dimers to resolve the questions posed above using the range of tools now available. As shown below, three dimers were prepared. HO_2C-***Dec-G(12***)-OH, a lower homologue of the known HO_2C-***Dod-G(12)***-OH was prepared using a solution phase route to ensure that the previously prepared sample was not active simply as a result of some impurity from the solid phase method. The fluorescently labelled equivalent HO_2C-***Dip-G(12)***-OH was prepared to provide a means to track the location of the transporter. Finally, a non-ionisable compound ***Prop-Dip-G(14)***-OH was prepared as a hydrophobic relative that would be expected to have a high affinity for a vesicle bilayer membrane, and therefore would provide a control compound for fluorescence-quenching studies; it was not expected to act as a channel.

*Corresponding author. Email: tmf@uvic.ca

ISSN 1061-0278 print/ISSN 1029-0478 online

http://dx.doi.org/10.1080/10610278.2011.622382
http://www.tandfonline.com

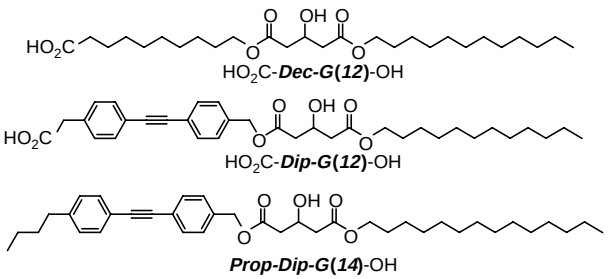

Results and discussion

Synthesis

The syntheses followed directly from previously developed modular methodology (*23*). The synthesis of HO_2C-***Dec-G(12)***-OH starts from the prenyl ester of 10-hydroxydecanoic acid (**1**) prepared from the previously reported *O*-tetrahydropyranyl derivative (*20*) (Scheme 1). Under standard ester coupling conditions to the known glutarate half-ester (**2**), **1** gave the protected diester **3** in good yield which was then doubly deprotected with TMS-triflate to give the target compound.

The synthesis of ***Prop-Dip-G(14)***-OH required the 4-butyl-4′-hydroxymethyldiphenyl acetylene (**4**) which was simply obtained via the Sonogashira coupling between the commercially available 1-bromo-4-butylbenzene and 4-ethynylbenzyl alcohol. Compound **4** reacted sluggishly with the protected hydroxyglutaric anhydride to give the expected glutarate half-ester **5** as a dark oil. Without purification, this was further coupled with tetradecanol (to yield **6**) and deprotected to give the desired compound in moderate yield.

The synthesis of HO_2C-***Dip-G(12)***-OH also begins with 4-ethynylbenzyl alcohol, which was then ester coupled to the aforementioned **2**. The resultant terminal alkyne **7** then underwent the Sonogashira coupling with the prenyl-protected 4-iodophenylacetic acid **8**. Simultaneous prenyl and tBDMS deprotection of the substituted diphenylacetylene **9** affords the final compound.

Both HO_2C-***Dip-G(12)***-OH and HO_2C-***Dec-G(12)***-OH had spectral features entirely in line with those of close relatives prepared previously (see Supplemental Information available online). HPLC purification of all three final compounds gave high-purity samples for subsequent studies.

Aggregation in aqueous solution

Previous work with other oligoester ion channels indicated the important role that aqueous phase aggregation plays in controlling their behaviours (*22*, *23*). Given that one of the core questions was whether or not HO_2C-***Dec-G(12)***-OH is ‘just a detergent’, we began by examining aggregation

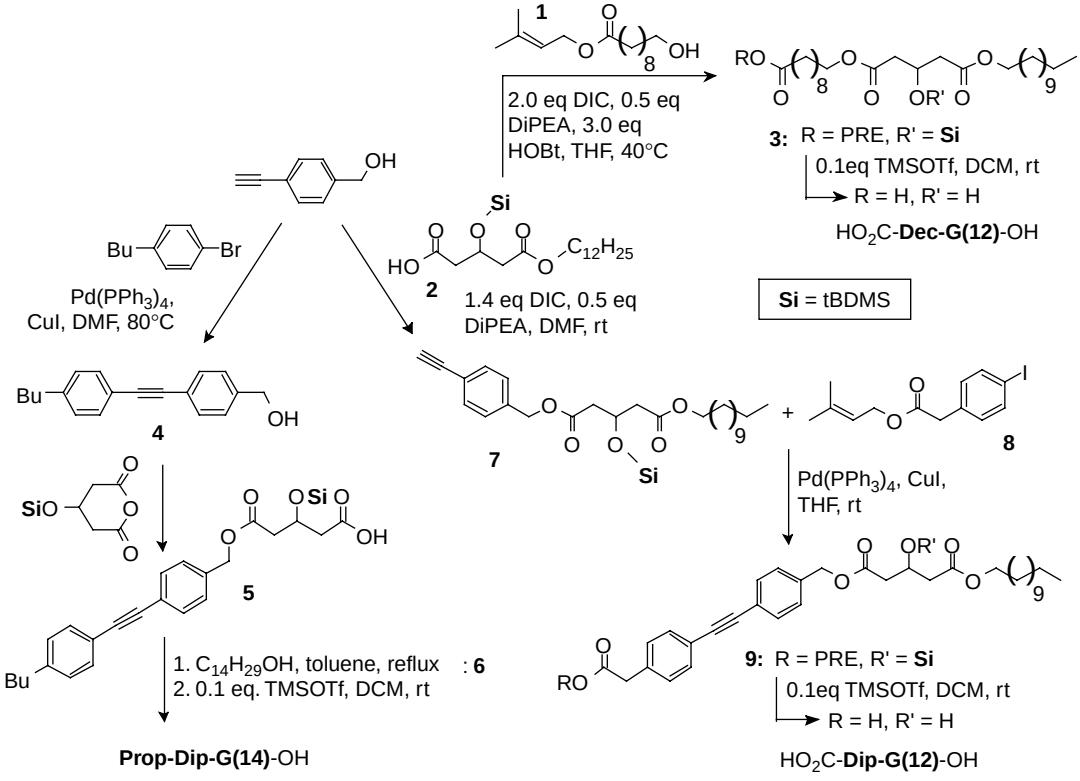

Scheme 1. Synthesis of 3-hydroxyglutarate diesters.

behaviour in aqueous solution using the pyrene assay method (*22*, *24*). In this assay, the emission spectrum of pyrene in water is recorded as a function of increasing concentration of compound. The ratio of the intensities of the first to the third vibronic bands (I_1/I_3) provides a measure of the polarity of the environment from a value of ca. 1.6 in water to ca. 1 in non-polar solution. A shift at a particular concentration of surfactant has been used to determine the cmc of conventional surfactants (*25*). The oligoester compounds studied previously are not typical surfactants but do show a change over a fairly broad concentration in the range of 10–50 μM; HO_2C-***Oct-Dec-Oct-G(10)***-OH is typical at 33 μM (*22*). Both HO_2C-***Dec-G(12)***-OH and HO_2C-***Dip-G(12)***-OH are significantly different with apparent cmc values in a range centred at 150 and 200 μM, respectively. The value for compound ***Prop-Dip-G(14)-***OH is 23 μM, in line with its neutral and weakly amphiphilic structure (see Supplemental Information available online). Thus under a typical concentration range for transport studies (10–60 μM), both HO_2C-***Dec-G(12)***-OH and HO_2C-***Dip-G(12)***-OH are likely monomeric in water.

Transport in vesicles

The transport activity was assessed using a vesicle-based assay in which a pH-sensitive dye (hydroxypyrene trisulfonate; HPTS) is used to report the collapse of a pH gradient imposed by an initial pulse of base outside the vesicle (*22*, *23*, *26*). Initial experiments were only weakly reproducible and it was found necessary to provide a 20-min delay period between injection of compound to the vesicles and initiation of transport via base injection. With this refinement in protocol, the transport results appear as illustrated in Figure 1. As expected, both HO_2C-***Dec-G(12)***-OH and HO_2C-***Dip-G(12)***-OH are active while ***Prop-Dip-G(14)-***OH is indistinguishable from the background. The active compounds show different concentration behaviours; HO_2C-***Dec-G(12)***-OH gives a regular and near linear increase in rate with concentration while HO_2C-***Dip-G(12)***-OH gives a sigmoidal profile similar to, but at higher concentration than, previously reported ***Dip*** containing oligoesters (*23*). The time course of the release differs as well; the rapid initial jump due to osmotic balance processes (*27*) is approximately constant with HO_2C-***Dec-G(12)***-OH, but increases steadily with HO_2C-***Dip-G(12)***-OH. Compound HO_2C-***Dec-G(12)***-OH shows a specific rate at 32 μM ($k_{32\mu M}$) of $(30 \pm 2) \times 10^4$ s^{-1}. The results were reproducible in duplicate, and between two batches of vesicles, with a difference of $k_{32\mu M}$ between trials of 11%. This value is in excellent agreement with the previously reported value for the shorter homologue HO_2C-***Oct-G(12)***-OH: $(29 \pm 4) \times 10^4$ s^{-1} (*20*). Concurrent assays with a control compound, HO_2C**-Oct-Dod-Oct-G(10)-**OH, gave a $k_{32\mu M}$ of $(8.5 \pm 5.1) \times 10^4$ s^{-1}, with the literature value reported as $(6.3 \pm 2.1) \times 10^4$ s^{-1} (*22*).

The sigmoidal profile of compound HO_2C-***Dip-G(12)***-OH does not support a full Hill analysis as the range is getting close to the point where aggregation and precipitation compete. Nonetheless, it is clear that a Hill coefficient much greater than 1 would be required to fit the data. At the reference concentration of 32 μM, HO_2C-***Dip-G(12)***-OH is approximately as active as HO_2C-***Dec-G(12)***-OH. However, the ***Dip*** compound does not require the 20-min incubation period for activity. This observation is consistent with the previously proposed hypothesis that the ***Dip*** accelerates partitioning to the bilayer (*23*). The

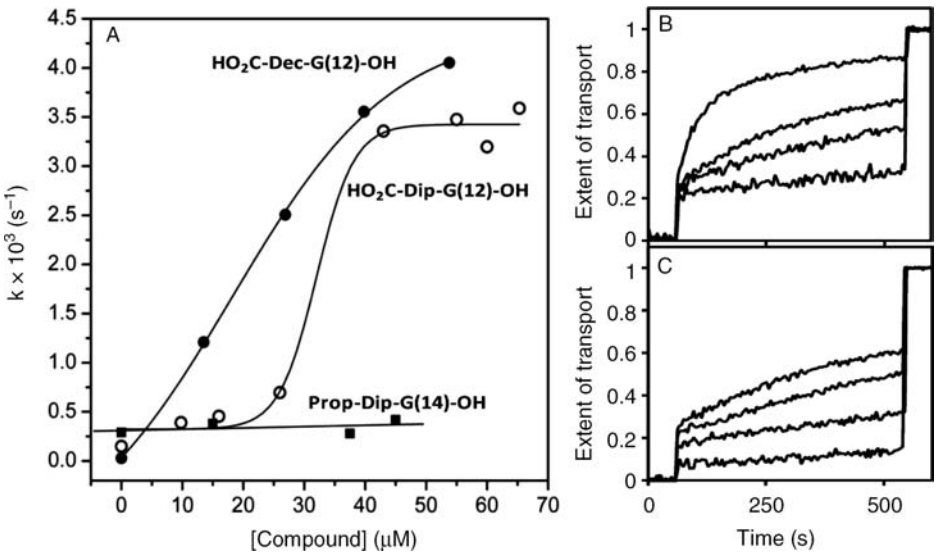

Figure 1. Transport by 3-hydroxyglutarate diesters in vesicles containing HPTS. Panel A – concentration dependence of the initial release rate. Time course of release by HO_2C-***Dec-G(12)***-OH (Panel B) and HO_2C-***Dip-G(12)***-OH (Panel C).

similarity of the rates suggests that there is relatively little difference between the channels that eventually form.

Leakage via detergent-like defects

An assay based on carboxyfluorescein (CF) is typically used to uncover the presence of large defects in a vesicle bilayer membrane (*28*). At a concentration above 10 mM, CF is self-quenched. Vesicles encapsulating CF at this concentration are orange and show only weak emission at 515 nm (475 nm excitation). In the presence of a compound that causes molecule-sized holes in the membrane, CF leaks into the external solution, is diluted, and the emission undergoes a significant increase in intensity. The assay involves incubation of CF-containing vesicles with increasing concentration of the putative disrupting agent, and uses a standard surfactant (Triton X100) as a control compound to establish the emission intensity at 100% release of CF. Remarkably, HO_2C-***Dec-G(12)***-OH was completely inactive in this assay in the range of 10–400 (see Supplemental Information available online); this is well into the range where the compound must be aggregated in aqueous solution, yet it remains incapable of forming large defects in vesicle bilayer membranes. Other saturated oligoester channel-forming compounds are somewhat more active (*29*); the control compound HO_2C**-Oct-Dod-Oct-G(10)-**OH gave 15% release at 105 μM and 35% release at 250 μM.

In contrast, HO_2C**-Dip-G(12)-**OH does provoke CF leakage with approximately 50% leakage at 50 μM (see Supplemental Information available online). This is in the range of the sharp increase in the transport rate assessed by the HPTS assay (above) and we take that as evidence that large holes can form in this concentration range. Note that this is still well below the concentration at which aqueous phase aggregation can be considered significant.

Transport in planar bilayer membranes

The formation of a conducting structure in a planar bilayer membrane is readily detected at the single molecule level using the voltage clamp technique (*6*, *30*). The bilayer is an insulator, and in the absence of an applied potential, no ionic current can flow. When a conducting structure opens, a sharp increase in conductivity is observed followed by a step back to the baseline. As illustrated in Figure 2, both HO_2C-***Dec-G(12)***-OH and HO_2C-***Dip-G(12)***-OH readily form conducting states in planar bilayers. The figure shows CsCl electrolyte, but activity was observed in KCl and NMe_4Cl contacting electrolytes as well. Not every experiment attempted resulted in conductance activity; the 'success' rate was approximately 50% for HO_2C-***Dec-G(12)***-OH and somewhat higher for HO_2C-***Dip-G(12)***-OH. As is obvious from Figure 2, these conductance events are not of the well-behaved step-on, step-off 'square top' type; the active compounds of this study only rarely show this type of activity. Rather, the conducting events have a clear 'on' and 'off' point, but the intervening conducting state shows a range of values, sometimes discrete, sometimes quite variable. This conductance profile indicates that there are a range of 'open' states that interconvert during the duration of the event (so-called multiple opening events). These two traces are representative of the range of conductance behaviours observed; the full set of data is available in summary form (see Supplemental Information available online).

The current–voltage profile of HO_2C-***Dec-G(12)***-OH is Ohmic, but the profile for HO_2C-***Dip-G(12)***-OH is clearly nonlinear at higher potentials as shown in Figure 2(E). The overall profile is symmetric indicating that the conducting state is not inherently rectifying. The data can be analysed as a linear (Ohmic) response between −75 and +75 mV having a specific conductance of 50 pS with an additional exponential increase in conductance corresponding to an *e*-fold increase every 25 mV. According to the Hille equation, which relates the observed conductance to channel dimensions using a continuum model (*6*, *30*), a specific conductance of 50 pS corresponds to a pore diameter of 0.2 nm. This is physically unrealistic as a Cs^+ has an ionic *radius* of 0.18 nm; all that can be stated is that the pores formed are very tight and likely dehydrating. An exponential increase in conductance of this type has been reported previously, but is a rare phenomenon (*31*). It would be consistent with a potential-dependent change in partitioning or orientation of HO_2C-***Dip-G(12)***-OH within the bilayer, or with an enlarging of the pore stabilised at higher potential. These are 'multiple opening' conductance states at the single-molecule level, thus any change due to potential will be manifest as the average behaviour of a set of conducting states active over the duration of the experimental potential scan. The specific molecular nature of the pores and their response to potential is therefore inaccessible by this technique, and the wide range of implied diameters make it unlikely that specific ionic selectivity can be identified.

We recently introduced a methodology for summarising the range of conductance behaviours observed within a voltage clamp trace using an activity grid to represent the duration of the conductance event (horizontal position on a log scale from 10 ms to 100 s), specific conductance of the event (vertical log scale in half log unit steps from 3 to 3000 pS) and colour shading to indicate the type of activity observed (green for regular step-like behaviour, blue for the majority 'multiple opening' behaviour illustrated in Figure 2, red for short duration spikes, grey regions of the grid where the experimental set-up precludes detection of events). Details and examples are developed elsewhere (*6*); note that greyscale and symbols are used in place of colour, but the meaning is the same as previously. Specific

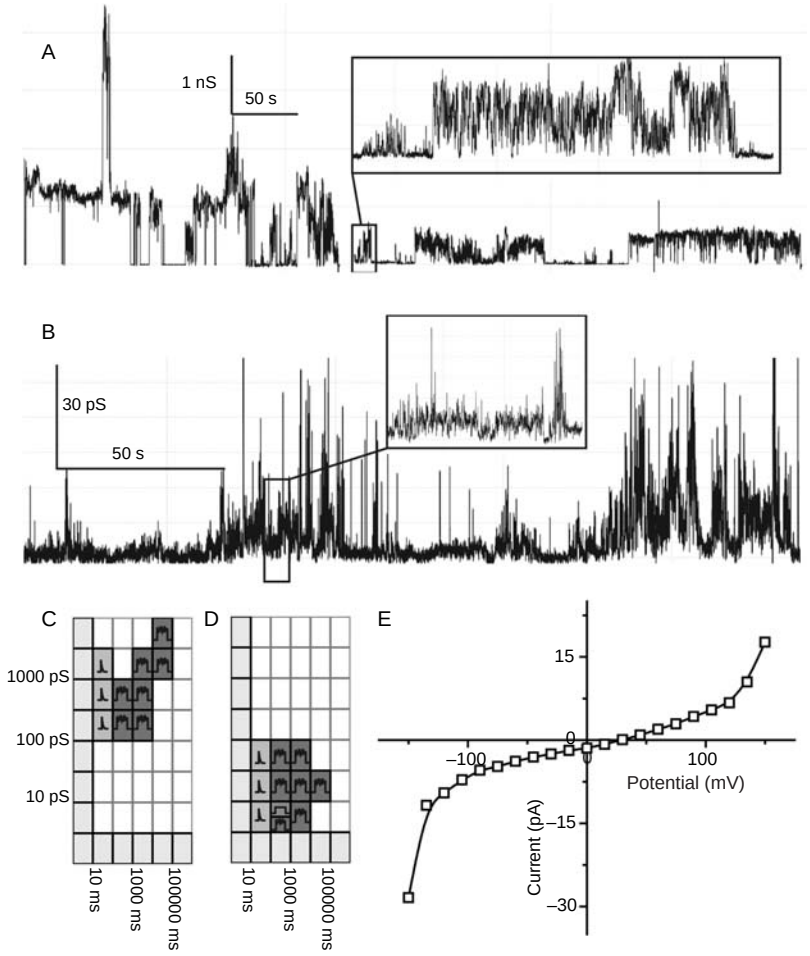

Figure 2. Bilayer conductance data for active compounds. (A) Conductance as function of time for HO_2C-***Dec-G(12)***-OH added from MeOH solution to diPhyPC bilayers in 1 M CsCl, pH 7, applied potentials from + 10 to − 75 mV; (B) Conductance as function of time for HO_2C-***Dip-G(12)***-OH added from MeOH solution to diPhyPC bilayers in 1 M CsCl, pH 7, applied potential initially + 150 mV switched to − 150 mV in the middle of this section; (C) HO_2C-***Dec-G(12)***-OH and (D) HO_2C-***Dip-G(12)***-OH: activity grids for the traces given; (E) current–voltage trace for HO_2C-***Dip-G(12)***-OH recorded approximately 5 min prior to the data of Panel B (applied potential cycled at 50 ms per potential, average of four cycles separated by approximately 10 s).

activity grids for the two traces given in Figure 2(C,D) show that at the coarse-grained level of the activity grids, these two compounds behave similarly with respect to the characteristics of the conductance profile, but that of HO_2C-***Dec-G(12)***-OH appears to be more highly conducting than HO_2C-***Dip-G(12)***-OH for this pair of records.

The entire body of experimental data was summarised using activity grids for each trace recorded and the collection was then summed to generate a set of cumulative activity grids as given in Figure 3. These cumulative activity grids show the types of activities observed, with the colour intensity representing the frequency of the observation within each type of observation. 'Multiple opening' (blue) and 'spike' (red) behaviours were observed in every trace while 'erratic' behaviours were observed in approximately 30% of the traces recorded. Regular 'square top' openings, although spread over a significant duration/conductance area of the activity grid, were very rare; they occur in only a few traces recorded for HO_2C-***Dip-G(12)***-OH and were never observed for HO_2C-***Dec-G(12)***-OH. The apparent difference in conductance and duration between the compounds shown in Figure 2 is only weakly supported by the cumulative data; the dominant cluster of 'multiple opening' events for HO_2C-***Dip-G(12)***-OH is somewhat below (lower conductance) and to the left (shorter duration) of the dominant cluster of the same type of event for HO_2C-***Dec-G(12)***-OH, but the statistical significance of this must be very weak.

If we treat the two compounds as closely similar, the predominant 'multiple opening' (blue) conductance state lies between 100 and 300 pS. According to the Hille equation this corresponds to a pore diameter in the range of 0.2–0.4 nm – still physically unrealistic for most ions. The 'erratic' conducting events (purple) appear at higher

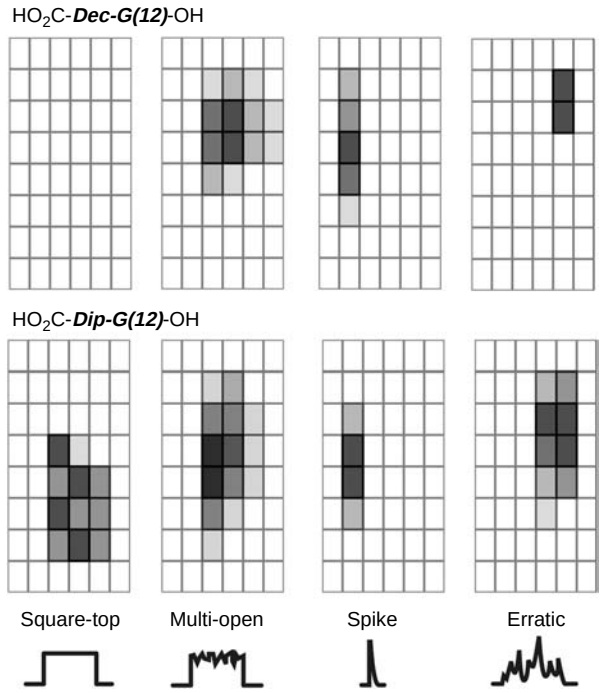

Figure 3. Cumulative activity grids for HO_2C-***Dec-G(12)***-OH (top) and HO_2C-***Dip-G(12)***-OH (bottom) separated by type of activity observed.

conductance (300–1000 pS) with an apparent pore diameter of 0.4–0.8 nm. Given the size of the compounds, such states must require many molecules to act together to stabilise a structure of this size. A large number of molecular orientations are therefore probable and the 'single molecule conductance' is therefore highly irregular. The diameter is, however, in the realm of physically realistic for the passage of ions, perhaps partly hydrated. Figure 3 also suggests a general tendency to longer lived states having higher conductances. This is evident in places in Figure 2(A,B) as well and appears to be general for many synthetic ion channels (*6*).

As a final point, the clustering evident in the summary activity grids is both in line with other synthetic ion channels (*6*) and inconsistent with a simple detergent disruption of the membrane. It is also qualitatively different from the reported behaviour of Triton X100 channels which are reported to involve predominantly 'square top' (green) events in the 30–100 pS conductance range in diPhyPC membranes (*6*, *18*, *19*).

Fluorescence

On excitation near 300 nm, diphenyl acetylenes show an emission from a monomeric state in the region of 320 nm and an excimer emission as a band of variable shape in the region of 360–380 nm (*32*, *33*). We have previously used this property to explore the distribution and interconversion of species during the transport process mediated by Dip-containing oligoesters (*23*). Both HO_2C-***Dip-G(12)***-OH and ***Prop-Dip-G(14)***-OH show the expected fluorescence properties as illustrated in Figure 4. In homogeneous solution in tetrahydrofuran (THF) or methanol, only monomer emission at 320 nm is observed. In aqueous solution, the predominant emission is from the excimer. This is in the range of concentrations at which ***Prop-Dip-G(14)***-OH shows evidence of aggregation, therefore, this is unsurprising for this compound. However, this is well below the concentration at which HO_2C-***Dip-G(12)***-OH shows evidence of aggregates capable of protecting pyrene from an aqueous environment. The observed excimer emission points to either dimers or very small aggregates that ignore pyrene as a guest. The aqueous solutions are not stable and the spectra evolve over time. Addition of vesicles abruptly alters the spectra from a predominant excimer emission to a predominantly monomer emission. The excimer emission slowly recovers intensity over time, a process that we have previously

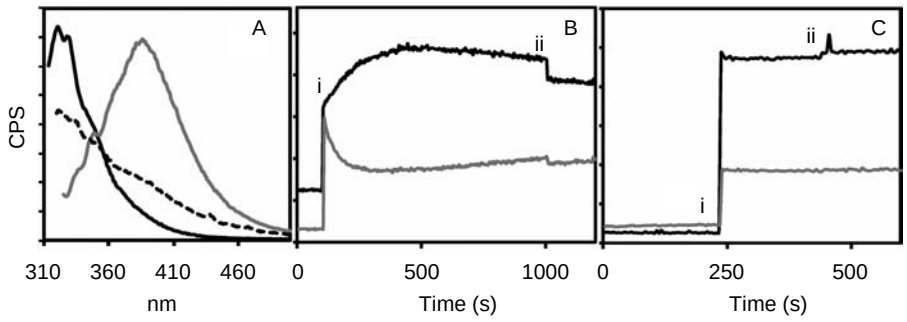

Figure 4. Fluorescence characteristics in differing media. (A) Fluorescence emission spectra of 28 μM HO_2C-**Dip-G(12)**-OH in MeOH (black solid line), aqueous buffer (grey solid line) and after incubation with lipid vesicles (black dashed line). Ex = 302 nm. (B) Emission over time at 320 nm (black line) or 380 nm (grey line) of an aqueous solution of 22 μM HO_2C-**Dip-G(12)**-OH to which vesicles (time = **i**) and $CuSO_4$ (time = **ii**) have been added. (C) Analogous data for 32.5 μM **Prop-Dip-G(14)**-OH, grey line = 361 nm, all other parameters are identical to B.

related to transfer of material from the aqueous aggregate to an aggregate in vesicles (*23*).

Diphenylacetylene fluorescence can be quenched with aqueous copper ion (*23*); the quenching constants are in the mM range for quenching monomer in homogeneous solution and in the μM range for quenching the excimer emission of an aqueous aggregate. In this respect, HO_2C-***Dip-G(12)***-OH behaves in an analogous fashion to other ***Dip***-containing oligoesters studied. With ***Prop-Dip-G(14)***-OH emission from the monomer being similarly quenched, but direct preparation of the aqueous aggregate results in only limited quenching of the excimer. We interpret this behaviour as consistent with a well-structured aggregate that lacks the surface charges that facilitate static quenching of the other compounds we have studied. The time-dependent emissions from vesicles in contact with the two compounds are illustrated in Figure 4(B,C). Addition of vesicles provokes rapid and significant changes in the spectra of both compounds, consistent with a significant partitioning of the compound from water to the vesicles. Later in the experiment, the addition of copper ion results in very limited quenching of species that have formed within the membrane. The overall conclusion is that the ***Dip*** component is within the membrane in an environment into which copper ions have little or no access. In both cases, the monomer signal is predominant in the presence of vesicles.

Conclusions

The central conclusion is clear: neither HO_2C-***Dec-G(12)***-OH nor HO_2C-***Dip-G(12)***-OH is 'just a detergent'; non-specific membrane lysis by detergent-like micelles is clearly refuted by experiment. The compounds are active in vesicle membranes at concentrations at which they are likely present as monomers in aqueous solution. The channels observed by the voltage clamp technique show a range of conducting structures, but at a coarse-grained level these appear to similarly cluster for the two compounds. There is evidence from fluorescence studies that aggregation may occur following partitioning, and this would be in line with previous mechanistic proposals. In this interpretation, the high activity observed for HO_2C-***Oct-G(12)***-OH previously and for HO_2C-***Dec-G(12)***-OH in this study is the result of a higher monomer concentration available to drive the compound into the membrane. Whatever the mechanism, it is also clear that these active compounds represent another example of minimalist ion channel-forming compounds.

But what are the conducting structures? All the evidence is indirect and only weakly restrains mechanistic speculations. However, there is an emerging picture from molecular dynamics simulations (*34*), membrane biophysics (*35*), structural determinations of barrel-stave and toroidal pores (*36*, *37*), and mechanistic studies of antimicrobial peptides (*38*) that the interaction of pore formers with lipids leads to a continuum of structures ranging from defects in which a line of waters can span a bilayer through defined barrel-stave structures in which a pore is lined by the pore former, via toroidal structures in which the pore former assists the lipid head groups to line a large pore, and eventually to detergent-like activity in which micellar structures are removed from the bilayer. Our data are consistent with this spectrum of activities. In this picture, the low-conductance openings would relate to the restricted water channel type, whereas higher conductance openings would be of the toroidal pore type and therefore more dynamic. A well-structured barrel-stave model is not as consistent with the data, as such a structure would be expected to report that the ***Dip*** units are in an active aggregate.

Experimental

Supplemental information available at http://hdl.handle.net/1828/3346: ^1H and ^{13}C NMR spectra of all compounds prepared, fluorescence data to support the experiments discussed and summary planar bilayer activities.

Synthesis

General procedures

Most chemicals and solvents were used as received from known suppliers, except tetrahydrofuran (THF) and dimethylformamide (DMF) which were dried and distilled before use. NMR spectra were collected at 300 or 500 MHz. UV spectra were run on a Cary 5 UV–Vis spectrometer in a 10 × 10 mm quartz cell. ESI mass spectra were recorded on a Waters MicroMass Q-TOF instrument (Milford, MA, USA) running in negative ion mode; MALDI spectra were recorded on a PerSeptiveBiosystemsVoyager – DE system (applied Biosystems, Boston, MA, USA). HPLC was performed using an HP Series 1100 instrument, with either a Macherey-Nagel 'Nucleosil' RP C18 analytical (4 mm × 250 mm) (Bethlehem, PA, USA) or a Grace Davison 'Alltima' RP C18 semi-prep (10 mm × 150 mm) column (Mandel Scientific, Guelph, ON, CA). Solvents used (ACN, CH_3OH; HPLC grade, H_2O; Milipore) were filtered through a Milipore sub-micrometre filter before use. HPLC elution was monitored at various UV wavelengths (typically 254, 280 and 220 nm) and fluorometrically ($\lambda_{ex} = 305$, $\lambda_{em} = 320$ nm). Fluorescence spectra were run on a PTI QM-2 instrument (Birmingham, NJ, USA) at $T = 20$°C in 10 × 10 mm quartz cells equipped with a micro stir rod or 1 × 10 mm quartz cells (no stir rod) for the pyrene and CF assays.

*Compound **3***

To a stirred solution of HO_2C-***G(12)***-OtBDMS (***2***) (*21*) (0.44 g, 1.02 mmol) in 8 mL of degassed THF, hydroxybenzotriazole (HOBt) (0.0621 g, 0.46 mmol) in 2 mL was

added. The reaction mixture was left to stir for 20 min under N_2 before the addition of di-isopropyl ethyl amine (DIPEA) (0.4 mL, 2.30 mmol) and DIC (1.6 mL, 0.01 mol). After an additional 20 min of stirring, ***1*** (*23*) (0.14 g, 0.5 mmol) in 1 mL THF was added. The reaction mixture was left to stir overnight at 40°C, after which the white precipitate was filtered by suction from the clear colourless filtrate. The filtrate was washed with H_2O, 1% $NaHCO_3$, brine, dried over Na_2SO_4, concentrated by rotary evaporation to a clear, slightly yellow oil that was dried under vacuum overnight. The crude product was chromatographed (EtOAc in hexanes, increase in 5% after every 100 mL collected) to yield ***3***, a clear colourless oil (0.268 g, 72%). NMR (300 MHz, $CDCl_3$) ^{1}H: 0.04 (s, 6H), 0.85–0.81 (br, 12H), 1.27–1.23 (br, 28H), 1.59 (t, 6H, $J = 9$ Hz), 1.68 (s, 3H), 1.73 (s, 3H), 2.26 (t, 2H, $J = 8$ Hz), 2.52 (d, 4H, $J = 6$ Hz), 4.55–3.96 (m, 4H), 4.53 (m, 3H), 5.34–5.28 (m, 1H). ^{13}C: −4.9, −4.6, 14.1, 17.8, 17.9, 22.6, 24.9, 25.6, 25.7, 25.9, 28.5, 29.1, 29.1, 29.2, 29.3, 29.3, 29.5, 29.5, 29.6, 31.9, 34.3, 42.5, 61.1, 64.6, 64.6, 66.3, 118.7, 138.8, 171.0, 173.8.

HO_2C-**Dec-G(12)-**OH**:** **3** (0.20 g, 0.30 mmol) was dissolved in 15 mL DCM under N_2. Trimethylsilyl triflate (TMSOTf), 0.8 μL, was added via syringe. The reaction mixture was stirred for 30 min, washed with H_2O (× 2) then brine, dried over Na_2SO_4, filtered and condensed under reduced pressure. The crude product was crystallised out of the resulting yellow oil with hexanes to yield HO_2C-***Dec-G(12)-***OH as a white powder (0.0976 g, 67%). Purification of the crude product was performed with reverse phase HPLC (semi-prep column, 1:1 MeOH:ACN mobile phase, UV–Vis detection at 220–280 nm, RT ~ 5 min). With evaporation, the product fraction yielded translucent crystals. NMR (300 MHz, $CDCl_3$) ^{1}H: 0.87 (t, 3H, $J = 8$ Hz), 1.30–1.26 (br, 28H), 1.65–1.58 (m, 6H), 2.34 (t, 2H, $J = 8$ Hz), 2.56–2.54 (br, 4H), 4.10 (t, 4H, $J = 6$ Hz), 4.45 (pentet, 1H, $J = 6$ Hz). ^{13}C: 11.9, 20.5, 22.5, 23.6, 23.7, 26.3, 26.8, 26.4, 26.9, 27.0, 27.2, 27.3, 27.4, 27.4, 29.7, 31.7, 38.5, 62.6, 62.8, 62.9, 169.7, 169.8, 177.0. MS (negative ESI TOF MS): Calculated for $C_{27}H_{49}O_7^-$: 485.3478 amu, Found: 485.342 amu.

*Compound **4***

CuI (400 mg, 2.1 mmol), 1-bromobutylbenzene (8.563 g, 40.1 mmol) and 4-ethynylbenzyl alcohol (3.540 g, 26.7 mmol) were dissolved in 25 mL DMF, the solution was deoxygenated with N_2, and $Pd(PPh_3)_4$ (243 mg, 0.210 mmol) was added and the mixture was heated and stirred at 80°C under N_2 overnight. This solution was worked up by diluting with ~500 mL EtOAc, washing with 100 mL of 1% EDTA solution, then with 100 mL of H_2O and then 100 mL of NaCl (aq) (sat'd), dried with sodium sulphate and the solvents were removed by a rotary evaporator and vacuum line to afford a brown solid. This was chromatographed on silica (3:1, hexanes:ethyl acetate) to afford an orange fluffy solid. Amount: 2.4 g, yield: 36%. NMR (300 MHz, $CDCl_3$) ^{1}H: 0.85 (q, 3H, $J = 7$ Hz), 1.28 (sextet, 2H, $J = 7$ Hz), 1.53 (q, 2H, $J = 8$ Hz), 2.55 (t, 2H, $J = 8$ Hz), 4.63 (s, 2H), 7.08 (d, 2H, $J = 8$ Hz), 7.27 (d, 2H, $J = 8$ Hz), 7.36 (d, 2H, $J = 8$ Hz), 7.44 (d, 2H, $J = 8$ Hz). ^{13}C: 13.9, 22.3, 33.4, 35.6, 65.0, 88.5, 89.7, 120.3, 122.8, 126.8, 128.5, 131.5, 131.7, 140.8, 143.4.

*Compound **5***

Compound **4** (2.264 g, 8.2 mmol) and 3-(*tert*-butyldimethylsilyloxy)glutaric anhydride (2.00 g, 8.2 mmol) were dissolved in toluene (80 mL). The solution was refluxed overnight to afford an orange solution. Upon inspection by TLC, the reaction was not complete and additional 3-(*tert*-butyldimethylsilyloxy)glutaric anhydride (400 mg) was added to the solution and the mixture left at reflux for 16 h. Upon removal of the solvent, the black oily product appeared to be reasonably pure by NMR and was used directly in the next step. Amount: 4.54 g, yield: 98%. NMR (300 MHz, $CDCl_3$) ^{1}H: 0.01 (m, 6H), 0.77 (m, 9H), 0.85 (q, 6H, $J = 7$ Hz), 1.24 (sextet, 2H, $J = 7$ Hz), 1.52 (q, 2H, $J = 7$ Hz), 2.55, (m, 6H), 4.50, (q, 1H, $J = 6$ Hz), 5.04 (m, 2H), 7.08 (d, 2H, $J = 8$ Hz), 7.24 (d, 2H, $J = 8$ Hz), 7.36 (d, 2H, $J = 8$ Hz), 7.43 (d, 2H, $J = 8$ Hz). ^{13}C NMR: −4.8, −4.9, 14.1, 17.9, 22.3, 22.7, 25.5, 25.6, 31.6, 33.4, 35.6, 39.2, 42.3, 52.1, 66.0, 88.3, 90.1, 120.2, 123.5, 128.1, 128.5, 131.5, 131.7, 135.5, 143.5, 170.6, 176.7.

*Compound **6***

The crude product **5** (1.482 g, ~2.91 mmol), HOBt (0.7145 g, 4.37 mmol) and DIPEA (1.36 mL, 7.28 mmol) were dissolved in dry THF (75 mL) and allowed to stir for 10 min under N_2 at which time DIC (0.747 mL, 4.37 mmol) was added. The solution was stirred for 10 min under N_2 and then 1-tetradecanol (1.00 g, 4.66 mmol) was added and the mixture was stirred under N_2 overnight. The solution was worked up by diluting with EtOAc (200 mL), washing with dilute $NaHCO_3$ (20 mL), H_2O (20 mL) and NaCl (aq) (sat'd) (20 ml). The organic solution was dried with sodium sulphate to afford an orange product. The product was chromatographed on silica using 2:1 DCM:hexanes as eluent to afford ***6*** as a colourless oil. Amount: 1.39 g, yield: 41%. NMR (300 MHz, $CDCl_3$) ^{1}H: 0.06 (m, 6H), 1.32 (m, 26H), 1.57 (m, 5H), 2.56 (d, 2H, $J = 6$ Hz), 2.61 (m, 4H), 4.04 (o, 2H, $J = 3$ Hz), 4.57 (q, 1H, $J = 6$ Hz), 5.11 (m, 2H), 7.16 (d, 2H, $J = 8$ Hz), 7.32 (d, 2H, $J = 8$ Hz), 7.44 (d, 2H, $J = 8$ Hz), 7.50 (d, 2H, $J = 8$ Hz). ^{13}C: −4.8, −4.9, 13.9, 14.1, 17.9, 22.3, 22.7, 25.6, 25.9, 28.6, 29.2, 29.3, 29.6, 29.6, 31.9, 33.4, 35.6, 42.5, 53.4, 64.7, 65.9, 66.3, 88.3, 90.0, 120.2, 123.5, 128.1, 128.5, 131.5, 131.7, 135.6, 143.5, 170.8, 171.0.

Prop-Dip-G(14)*-OH**: Compound ***6 (0.300 g, 0.638 mmol) was dissolved in DCM (10 mL) and TMS–triflate (10 μL, 0.0319 mmol) was added. The mixture was stirred for 1 h and quenched and washed with water (3 × 20 mL) to form a colourless solution and then with NaCl (aq) (sat'd) (20 mL). The organic extract was dried with sodium sulphate and the solvent was removed by rotary evaporation to produce a solid. This was further purified by trituration via sonicating in hexanes and vacuum filtering to produce a white solid which was further purified by HPLC. Amount: 0.130 g, yield: 53%. NMR (300 MHz, $CDCl_3$) ^{1}H: 0.81 (t, 3H, $J = 7$ Hz), 0.86 (t, 3H, $J = 7$ Hz), 1.18 (m, 23H), 1.53 (m, 4H), 2.48 (d, 2H, $J = 6$ Hz), 2.55 (m, 4H), 4.03 (t, 2H, $J = 6$ Hz), 4.41 (q, 1H, $J = 6$ Hz), 5.09 (s, 2H), 7.09 (d, 2H, $J = 8$ Hz), 7.25 (d, 2H, $J = 8$ Hz), 7.37 (d, 2H, $J = 8$ Hz), 7.44 (d, 2H, $J = 8$ Hz). ^{13}C: 13.9, 14.1, 22.3, 22.7, 25.9, 28.5, 29.3, 29.5, 29.6, 29.6, 31.9, 33.4, 35.6, 40.6, 40.7, 64.7, 65.1, 66.1, 88.3, 90.2, 120.2, 123.6, 128.1, 128.5, 131.5, 131.7, 135.4, 143.5, 171.4, 171.9. MS (MALDI): [590.4(10%), 613.4(87%), 629.4(65%)]. Other notable peaks [637.3(60%), 659.3(84%, 675.3(100%)].

*Compound **7***

One equivalent (70 mg, 0.53 mmol) of 4-ethynylbenzyl alcohol was added to 1.4 equivalents of ***2***, 1.4 equivalents of DIC and 0.5 equivalents of DIPEA in DMF. The reaction mixture was stirred at room temperature for 16 h, after which was diluted with EtOAc, washed with H_2O, $NaHCO_3$ (sat) and NaCl (sat), dried over sodium sulphate and concentrated under vacuum. Purification by silica gel chromatography (elution at ~3% EtOAc/hexanes) yielded 196 mg (68%) of the target compound as a pale yellow oil. NMR (300 MHz, $CDCl_3$): ^{1}H: 0.02 (s, 3H), 0.04 (s, 3H), 0.82 (s, 9H), 0.87 (t, 3H, $J = 6$ Hz), 1.25 (s, 18H), 1.65–1.55 (m, 2H), 2.53 (d, 2H, $J = 6$ Hz), 2.60 (d, 2H, $J = 6$ Hz), 3.07 (s, 1H), 4.03 (m, 2H), 4.55 (p, 1H, $J = 6$ Hz), 5.09 (m, 2H), 7.29 (d, 2H, $J = 8$ Hz), 7.46 (d, 2H, $J = 8$ Hz). ^{13}C: −5.0, 14.1, 17.9, 22.7, 25.6, 25.9, 28.5, 29.2, 29.3, 29.5, 29.5, 29.6, 31.9, 42.4, 42.5, 64.7, 65.7, 66.3, 77.6, 83.2, 122.0, 127.9, 132.3, 136.5, 170.7, 170.9.

*Compound **8***

To a solution of 1.0 equivalent (1.29 g, 4.92 mmol) of 4-iodophenylacetic acid in ACN 2.0 equivalents HOBt, 2.0 equivalents DIC and 3 equivalents of DIPEA were added, and the reaction mixture was allowed to stir at room temperature for 30 min. After this time, 2.0 equivalents (1.05 mL) of prenyl alcohol was added, and the reaction mixture was continued to stir at room temperature for 16 h. After this time, the reaction mixture was diluted with EtOAc, washed with H_2O, $NaHCO_3$ (sat) and NaCl (sat), dried over sodium sulphate and concentrated under vacuum. Further purification by silica gel chromatography (elution at 10% EtOAc/hexanes) yields 1.44 g (84%) of **8** as white crystals. MP = 42–44°C. NMR (300 MHz, $CDCl_3$): ^{1}H: 1.68 (s, 3H), 1.74 (s, 3H), 3.54 (s, 2H), 4.58 (d, 2H, $J = 7$ Hz), 5.36 (m, 1H), 7.02 (d, 2H, $J = 8$ Hz), 7.63 (d, 2H, $J = 8$ Hz). ^{13}C: 18.0, 25.8, 40.8, 61.9, 92.6, 118.3, 131.3, 133.7, 137.6, 139.4, 171.0.

*Compound **9***

1.0 equivalent (171 mg, 0.31 mmol) of **7**, 1.3 equivalents (150 mg) of **8**, 5 mol% (18 mg) $Pd(PPh_3)_4$, 10 mol% (58.9 mg) CuI and 2.0 equivalents NEt_3 were added to dry, deoxygenated THF. The reaction mixture was stirred at room temperature for 16 h, after which it was diluted with EtOAc, extracted twice against saturated EDTA, washed once with H_2O and once with NaCl (sat), dried over sodium sulphate and concentrated under vacuum. Silica gel chromatography (elution at ~15% EtOAc/hexanes) yielded 142 mg (61%) of the target compound as a brown oil. NMR (300 MHz, $CDCl_3$): ^{1}H: 0.04 (s, 3H), 0.05 (s, 3H), 0.82 (s, 9H), 0.86 (t, 3H, $J = 6$ Hz), 1.24 (s, 18H), 1.62–1.57 (m, 2H), 1.68 (s, 3H), 1.74 (s, 3H), 2.54 (d, 2H, $J = 6$ Hz), 2.61 (d, 2H, $J = 6$ Hz), 3.61 (s, 2H), 4.03 (m, 2H), 4.59–4.52 (m, 3H), 5.10 (m, 2H), 5.32 (m, 1H), 7.27 (d, 2H, $J = 8$ Hz), 7.31 (d, 2H, $J = 8$ Hz), 7.48 (m, 4H). ^{13}C: −4.9, 14.1, 17.9, 18.0, 22.7, 25.6, 25.8, 25.9, 28.5, 29.2, 29.3, 29.4, 29.5, 29.6, 31.9, 41.3, 42.4, 42.5, 61.9, 64.7, 65.8, 66.3, 89.0, 89.6, 118.3, 121.9, 123.2, 128.1, 129.3, 131.7, 131.7, 134.4, 135.8, 139.4, 170.8, 171.0, 171.2.

*HO_2C-**Dip-G(12)**-OH*

1.0 equivalent (125 mg, 0.17 mmol) of **9** and 15% (~10 μL) TMSOTf were dissolved in 5 mL DCM. The reaction mixture was stirred for 10 min at room temperature, then diluted with DCM, washed with H_2O, NaCl (sat), dried over sodium sulphate and rotary evaporated. The obtained beige solid was then sonicated with hexanes and filtered, yielding 70 mg (73%) of **HO_2C-Dip-G(12)-**OH as a white solid. This was then purified by HPLC (semi-prep column, 75% ACN:CH_3OH, retention time ~4 min) to yield white crystals. UV (CH_3OH); λ_{max}Abs = 287 nm. Fluorescence (CH_3OH); λ_{max}-Ex = 302 nm, λ_{max}Em = 320 nm. NMR: ^{1}H (300 MHz, $CDCl_3$): 0.87 (t, 3H, $J = 7$ Hz), 1.25 (s, 18H), 1.64 (m, 2H), 2.54 (d, 2H, $J = 7$ Hz), 2.61 (d, 2H, $J = 7$ Hz), 3.67 (s, 2H), 4.09 (t, 2H, $J = 7$ Hz), 4.48 (p, 1H, $J = 6$ Hz), 5.15 (s, 2H), 7.27 (d, 2H, $J = 8$ Hz), 7.32 (d, 2H, $J = 8$ Hz), 7.50 (m, 4H). ^{13}C (125 MHz, 1:1, $CDCl_3$:MeOD): 15.7, 24.6, 27.8, 30.5, 31.2, 31.3, 31.4, 31.5, 31.5, 31.6, 33.8, 43.4, 66.8, 66.9, 67.9, 90.8, 91.5, 123.8, 125.3, 130.0, 131.4, 133.6, 133.6, 137.1, 137.9, 173.5, 173.9. MS

(negative ESI TOF MS): Calculated for $C_{34}H_{43}O_7$ = 563.3009 amu, obtained = 563.3237 amu.

Vesicle preparation and fluorimetry-based assays

All assays were based on procedures previously published (*22, 23*). The compound HO_2C-**Oct-Dod-Oct-G(10)**-OH (*22*) was used as a reference sample for all assays as a stock MeOH solution.

CF assay: vesicle preparation

Modified from published procedures (*28*): 0.45 g 5(6)-CF was added to ~5 mL deionised water, solvated by titration of 1 M potassium hydroxide to pH 7.5 (to form K^+CF^-), evaporated *in vacuo* and further dried under vacuum for 48 h. The CF salt was diluted with CF buffer (10 mM Tris·HCl, 0.04 M KCl in deionised H_2O), to KCF solution of 0.1 M (10 mL; pH 7.5 with 1 M HCl). To a 50 mL round-bottomed flask, 4 mL of lipid stock (8:1:1, PC:PA:cholesterol in $CHCl_3$) was dried under vacuum. The lipid was re-suspended in diethyl ether (6 mL) and 2 mL of the KCF solution was then added. Sonication was used to disperse the two phases to a cloudy orange dispersion (power = 2.5, probe tip at the interface of the two phases). This dispersion was evaporated slowly under vacuum until bubbling from ether removal stopped. Then, 1 mL external buffer (10 mM Tris·HCl, 0.14 M KCl in deionised H_2O, pH 7.5, with HCl) was added. Slow rotary evaporation of the suspension continued to remove any excess ether for 30 min. The liposomes were sized with the membrane extrusion apparatus 19 times (500 μL vesicle solution × 3) and then size exclusion filtered as noted. The cloudy fraction, after the first four cloudy drops, was collected, for a total volume of vesicle suspension of ~1.5 mL. The diameter of the resulting vesicles was ~200 nm (measured by dynamic light scattering). The vesicle solution was stored at 5 °C and used within 12 h.

Typical experiment

One hundred and sixty microlitre external buffer (10 mM Tris·HCl, 0.14 M KCl, pH 7.5) and 30 μL test solution (compound in THF or MeOH or 5% Triton X-100) were added to a 1.5 mL Eppendorf tube and vortexed briefly. To each tube, 20 μL CF vesicle suspension was added, vortexed for 10 s, and allowed to incubate at room temperature for 30 min. Each sample was then diluted to 5% in external buffer (1.5 mL total volume, 0.6 mL solution was used for each trial). Samples were excited at 475 nm (slits = 2 nm, integration = 1 s) and the fluorescence emission scan was measured from 500 to 550 nm in a 1 × 10 mm quartz cell at T = 20°C. The average emission intensity at λ_{max} (~515 nm) was determined for each sample concentration. The percentage of CF released was calculated as $I(\%) = [(I_{sample} - I_{MeOHblank})/(I_{triton} - I_{blank})$ and plotted against test compound concentration.

Bilayer clamp experiment

The methodology was derived from that previously described (*39*). A model BC-525A bilayer clamp (Warner Instrument Corp., Hamden, CT, USA) was used for all planar bilayer experiments; ClampEx 8 and ClampFit 10 (Axon Instruments – Molecular Devices, Sunnyvale, CA, USA) were the software used for acquisition and analysis, respectively. Cups used were made of polystyrene and had 250 μm diameter apertures. The lipid used in all cases was diphytanoylphosphatidylcholine (diPhyPC; Avanti Polar lipids). A stock solution of 25 mg/mL lipid in $CHCl_3$ was dried under N_2 and then re-suspended in 200 μL decane. For compounds that had to be pre-loaded into the lipid, 0.1–1 mol% compound in $CHCl_3$ was added to the lipid mix and then dried. The electrolytes used were 1 M KCl, CsCl or NMe_4Cl in 10 mM HEPES, 10 mM TRIS, pH 7 (unadjusted).

The aperture was primed with 0.5–1 μL of decane/lipid, excess solvent was removed by blowing N_2 over the aperture. The cup was then placed into the electrolyte-filled holding cell, consisting of 5 and 3 mL chambers, and salt bridges (KNO_3/Agar) and electrodes (Ag/AgCl) were attached. Bilayers were formed by brushing on 1–1.5 μL of the decane/lipid mixture over the aperture, and were monitored for stability, capacitance and resistance for at least 20 min before test compound was added. Test compounds were added by injection from an organic solution (typically no more than 1–10 μL of solution), or by breaking the lipid-only bilayer and brushing on the compound-preloaded in a lipid mix. All data were hardware filtered (eight-pole Bessel filter, 1 kHz) and data were collected in a survey mode using the Gap-free protocol. Bilayers were tested repeatedly for capacitance and resistance. Once formed, 'activity' from pristine bilayers was never observed.

Acknowledgements

The ongoing support of the Natural Sciences and Engineering Research Council of Canada and of The Nora and Mark DeGoutiere Memorial Scholarship (JMM) is gratefully acknowledged.

Note

1. 'The trivial naming of the compounds follows from the linear structures with the carboxy and hydroxy termini explicity specified; named subunits are assumed to be linked as esters. The **G(n)** unit indicates a diester of 3-hydroxyglutaric acid with an n-carbon alkyl ester, the esters of α,ω-hydroxyalkanoic acids of 8, 10, and 12 carbons as Oct, Dec, and Dod, and the ester of 4-carboxymethyl-4' hydroxymethyl-diphenylacetylene as Dip. In this paper only the final structures are named this way

References

(1) Fyles, T.M.; van Straaten-Nijenhuis, W.F. In Ion channel models. *Comprehensive Supramolecular Chemistry*; Reinhoudt, D.N., Ed.; Elsevier Science: Amsterdam/ New York, 1996; Vol. 10, pp 53–77.

(2) Sisson, A.L.; Shah, M.R.; Bhosale, S.; Matile, S. *Chem. Soc. Rev.* **2006**, *35*, 1269–1286.

(3) Davis, A.P.; Sheppard, D.N.; Smith, B.D. *Chem. Soc. Rev.* **2007**, *36*, 348–357.

(4) Gokel, G.W.; Carasel, I.A. *Chem. Soc. Rev.* **2007**, *36*, 378–389.

(5) Sansone, F.; Baldini, L.; Casnati, A.; Ungaro, R. *New J. Chem.* **2010**, *34*, 2715–2728.

(6) Chui, J.K.W.; Fyles, T.M. *Chem. Soc. Rev.* **2011**, DOI: 10.1039/c1cs15099e.

(7) Matile, S.; Vargas, A.; Montenegro, J.; Fin, A. *Chem. Soc. Rev.* **2011**, *40*, 2453–2474.

(8) Li, X.; Shen, B.; Yao, X.-Q.; Yang, D. *J. Am. Chem. Soc.* **2009**, *131*, 13676–13680.

(9) Li, X.; Shen, B.; Yao, X.-Q.; Yang, D. *J. Am. Chem. Soc.* **2007**, *129*, 7264–7265.

(10) Leevy, W.M.; Weber, M.E.; Gokel, M.R.; Hughes-Strange, G.R.; Daranciang, D.D.; Ferdani, R.; Gokel, G.W. *Org. Biomol. Chem.* **2005**, *3*, 1647–1652.

(11) Leevy, W.M.; Huettner, J.E.; Pajewski, R.; Schlesinger, P.H.; Gokel, G.W. *J. Am. Chem. Soc.* **2004**, *126*, 15747–15753.

(12) Mora, F.; Tran, D.-H.; Oudry, N.; Hopfgartner, G.; Jeannerat, D.; Sakai, N.; Matile, S. *Chem. Eur. J.* **2008**, *14*, 1947–1953.

(13) Litvinchuk, S.; Sorde, N.; Matile, S. *J. Am. Chem. Soc.* **2005**, *127*, 9316–9317.

(14) Kobuke, Y.; Ueda, K.; Sokabe, M. *J. Am. Chem. Soc.* **1992**, *114*, 7618–7622.

(15) Renkes, T.; Schafer, H.J.; Siemens, P.M.; Neumann, E. *Angew. Chem. Int. Ed. Eng.* **2000**, *39*, 2512–2516.

(16) Fyles, T.M.; Knoy, R.; Müllen, K.; Sieffert, M. *Langmuir* **2001**, *17*, 6669–6674.

(17) Yamnitz, C.R.; Negin, S.; Carasel, I.A.; Winter, R.K.; Gokel, G.W. *Chem. Comm* **2010**, *46*, 2838–2840.

(18) Rostovtseva, T.K.; Bashford, C.L.; Lev, A.A.; Pasternak, C.A. *J. Membrane Biol.* **1994**, *141*, 83–90.

(19) Schlieper, P.; De Robertis, E. *Arch. Biochem. Biophys.* **1977**, *184*, 204–208.

(20) Fyles, T.M.; Hu, C.; Luong, H. *J. Org. Chem.* **2006**, *71*, 8545–8551.

(21) Luong, H.; Fyles, T.M. *Org. Biomol. Chem.* **2009**, *7*, 725–732.

(22) Luong, H.; Fyles, T.M. *Org. Biomol. Chem.* **2009**, *7*, 733–738.

(23) Moszynski, J.; Fyles, T.M. *Org. Biomol. Chem.* **2010**, *8*, 5139–5149.

(24) Kalyanasundaraman, K.; Thomas, J.A. *J. Am. Chem. Soc.* **1977**, *99*, 2039–2044.

(25) Yihwa, C.; Kellermann, M.; Becherer, M.; Hirsch, A.; Bohne, C. *Photochem. Photobiol. Sci.* **2007**, *6*, 525–531.

(26) Matile, S.; Sakai, N. In The characterization of synthetic ion channels and pores. *Analytical Methods in Supramolecular Chemistry*; Schalley, C.A., Ed.; Wiley -VCH: Weinheim, 2007; pp 381–418.

(27) Kuyper, C.L.; Kuo, J.S.; Mutch, S.A.; Chiu, D.T. *J. Am. Chem. Soc.* **2007**, *128*, 3233–3240.

(28) Fyles, T.M.; Hu, C. *J. Supramol. Chem.* **2001**, *1*, 207–215.

(29) Luong, H.L. *Towards Voltage-Gated Channels Synthesized by Solid-Phase Methods*; University of Victoria: Victoria, 2008.

(30) Hille, B. *Ionic Channels of Excitable Membranes*;, 3rd ed. Sinauer Associates, Incorporated: Sunderland, 2001; p 383.

(31) Sakai, N.; Ni, C.; Bezrukov, S.M.; Matile, S. *Bioorg. Med. Chem. Lett.* **1998**, *8*, 2743–2746.

(32) Hirata, Y. *Bull. Chem. Soc. Jpn* **1999**, *72*, 1647–1664.

(33) Letsinger, R.L.; Wu, T.; Yang, J.-S.; Lewis, F.D. *Photochem. Photobiol. Sci.* **2008**, *7*, 854–859.

(34) Fuertes, G.; Gimenez, D.; Esteban-Martin, S.; Sanchez-Munoz, O.; Salgado, J. *Eur. Biophys. J.* **2011**, *40*, 399–415.

(35) Heimberg, T. *Biophys. Chem.* **2010**, *150*, 2–22.

(36) Qian, S.; Wang, W.; Yang, L.; Huang, H.W. *Biophys. J.* **2008**, *94*, 3512–3522.

(37) Qian, S.; Wang, W.; Yang, L.; Huang, H.W. *Proc. Natl. Acad. Sci. USA* **2008**, *105*, 17379–17383.

(38) Wimley, W.C. *ACS Chem. Biol.* **2010**, *5*, 905–918.

(39) Eggers, P.K.; Fyles, T.M.; Mitchell, K.D.D.; Sutherland, T. *J. Org. Chem.* **2003**, *68*, 1050–1058.